

Analysis on Geo-stress and casing damage based on fluid-solid coupling for Q9G3 block in Jibei oil field

Youjun Ji^{*1,2,3,4} and Xiaoyu Li^{1,3}

¹Sichuan Key Laboratory of Natural Gas Geology, Southwest Petroleum University, Chengdu, China

²Ecological Security and Protection Key Laboratory of Sichuan Province, Mianyang Normal University

³School of Geoscience and Technology, Southwest Petroleum University, Chengdu, China

⁴State Key Laboratory of Reservoir Geology and Development Engineering, Southwest Petroleum University, Chengdu, China

(Received July 21, 2016, Revised November 12, 2017, Accepted November 17, 2017)

Abstract. Aimed at serious casing damage problem during the process of oilfield development by injecting water, based on seepage mechanics, fluid mechanics and the theory of rock mechanics, the multi-physics coupling theory was also taken into account, the mathematical model for production of petroleum with water flooding was established, and the method to solve the coupling model was presented by combination of Abaqus and Eclipse software. The Q9G3 block in Jibei oilfield was taken for instance, the well log data and geological survey data were employed to build the numerical model of Q9G3 block, the method established above was applied to simulate the evolution of seepage and stress. The production data was imported into the model to conduct the history match work of the model, and the fitting accuracy of the model was quite good. The main mechanism of casing damage of the block was analyzed, and some wells with probable casing damage problem were pointed out, the displacement of the well wall matched very well with testing data of the filed. Finally, according to the simulation results, some useful measures for preventing casing damage in Jibei oilfield was proposed.

Keywords: casing damage; seepage mechanics; fluid-solid coupling; mathematical model; numerical analysis

1. Introduction

The casing damage is a very serious problem in many oilfields in China and other countries in the world (Ren *et al.* 2010). According to literature research at home and abroad for nearly 30 years, it is found that the casing damage is a long-term problem which has not been solved well.

Since the 1970s, the casing damage is a very serious problem in China. By statistics data (Diao *et al.* 2008), the number of the casing damage well had reached more than 14000, including Daqing, Jilin, Dagang, Huabei, Zhongyuan, Jianghan, Xinjiang, Yumen, Shengli, Sichuan and Liaohe oilfield. If the cost of each well is RMB 1.5 million, the direct economic loss of casing damage is as high as RMB 21 billion each year. However, this does not include the economic loss caused by stopping production. With the application of various kinds of measures to increase oil recovery factor, the casing damage problem in china is becoming more and more serious. The situation in foreign countries is the same, such as the west Siberian oil field, the north Caucasus oil field and so on. Casing damage is often encountered and inevitable in the process of oilfield development, which brings a lot of loss to normal production of oilfield. Therefore, it is currently in an urgent need to solve in the world.

For oilfield exploitation by water injection, water flooding has changed the initial geological environment of reservoir and breaks the balance of geo-stress (Huang *et al.* 2008). By the research work of Bu (2011), the migration of injected water and crude oil in the reservoir affect the stress and deformation field. According to Ai's (2003) research, the injected water also has impact on mechanical properties of mudstone. If injected water flow into the fault, it will trigger fault slip (Wu *et al.* 2005). All of these processes above make the geological conditions of reservoir very complex, also the pressure on the casing pipe, and hence the stress on the well is very difficult to analyze. Usually, it is impossible to predict the casing damage by direct method, such as experiment, stress survey on the spot, the most popular and effective method is numerical simulation (Han *et al.* 2006).

Through analysis on failure mechanism of casing and simulating the stress and how the casing is damaged, and then put forward some measures to prevent casing damage constitute the main content for the research of casing damage by numerical method (Cui *et al.* 1994). The direct observation for causing damage can be executed through various kind of modern technology, and mechanism of casing damage can be quantitatively analyzed by using the finite element method. However, there still exist many problems in the study on mechanism of casing damage. Based on elastic-plastic mechanics and rock rheology mechanics, physical and numerical simulation method are used to study damage of casing (Liu *et al.* 2008). However, there are few literatures about study on the influence of fluid in reservoir on casing damage, it is also called

*Corresponding author, Associate Professor
E-mail: jyyoujun0319@163.com

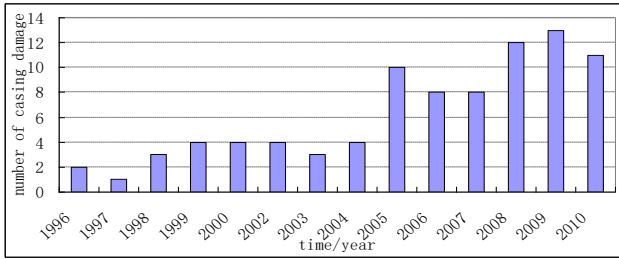


Fig. 1 The number of well with casing damage problem each year

coupling effect of seepage and deformation. The influence of seepage in reservoir on the stress should not to be ignored during the analysis of casing damage, sometimes, even it plays very important role in the casing damage (Zhu and Gu 2013).

Research work about prediction and prevention of casing damage involves the structural geology, earth dynamics, rock mechanics, material mechanics, elastic-plastic mechanics, etc. (Raouf *et al.* 2016). At the same time, it also involves the numerical method, the material and geometric nonlinear theory, and computation science (Wang *et al.* 2011). This study has penetrated into the mechanics, mathematical and physical sciences theory, it is comprehensive and include cross discipline (Cheng *et al.* 2013). It is difficult to simulate complex geo-stress and deformation process of reservoir formation only through physical experiment. Therefore, numerical simulation technology with computer becomes the main method for study of stress in oilfield and the research trend of this area.

Until now, there are 315 wells in Jibei oilfield, 273 of which are opened and 42 are closed. The total number of injection well is 112, 83 of which are opened and 29 are closed. Among these wells, casing damage has happened to 91 of them, 60 of which are oil production well and 31 are water injection.

The mode of casing damage in Jibei oilfield mainly includes deformation of casing, extrusion, shear and tensile failure, from the statistical data of broken well, the number of well in the mode of deformation and extrusion failure is 68, which takes up 74.7%, the number of deformation is 15, which takes up 16.5%, the number of faulted well caused by shearing failure is 8 and takes up 8.8%. Fig. 1 indicates the number of well with casing damage problem vs. time.

For the situation above, this study focused on the establishment of mechanical model based on fluid-solid coupling. By numerical simulation of the production history of Q9G3 block in Jibei oilfield, the influence of injection-production parameters on geo-stress and mechanism of casing damage were analyzed. Combined with the dynamic change of information database, the warning information of casing damage is given out through numerical analysis on the geostress and the pressure on the casing pipe. The work of this study would provide the basis for preventing casing damage and prolonging the life of the production well.

2. Fluid-solid coupling model for water flooding process

2.1 Seepage mechanics model

For the fluid flowing in reservoir development with water flooding method, it involves migration of water and oil phase. With the development of field, there exists not only flowing of multiphase fluid, but also phase transition, it is a very complex process. Because we just discuss the influence of fluid flowing on the stress in reservoir, the mathematical model can be described with the Black Oil model (Yin *et al.* 2004). At the same time, in order to simplify the calculation process, capillary pressure is also ignored during the two phase flow of water and oil. It means that p_o equals p_w and p_w equals p_o . When the deformation characteristic of porous media is taken into account, the seepage equation for flowing of two phase fluid is as follows

$$\nabla \left[\frac{KK_{rm}}{\mu_m} (\nabla p - \rho_m g \nabla D) \right] + \varphi C_m S_m B_m \frac{\partial p}{\partial t} + \varphi \frac{\partial S_m}{\partial t} + \frac{S_m(1-\varphi_0)}{(1+\varepsilon_v)^2} \frac{\partial \varepsilon_v}{\partial t} + \frac{q_m}{\rho_m} = 0 \quad (1)$$

where $m=o, w$, μ_m is the viscosity of the fluid, mPa·s; q_m is the production of oil or water, m³/day; S_m is saturation of the fluid; p is the pore pressure of the fluid, kPa; K is the permeability, 10⁻³μm²; K_{rm} is the relative permeability of the fluid; ρ_m is the density of the fluid, kg/m³; g is gravitational acceleration, m/s²; D is the relative elevation, m; C_m is the compressibility of the fluid, kPa⁻¹; B_m is volume factor of the fluid; t is the time; φ is the porosity of formation; φ_0 is the initial porosity of formation; ε_v is the volume strain.

2.2 The model of stress field

According to Terzaghi's principle of effective stress (Koltuk *et al.* 2013), the external load acting on the saturated rock composed of porous media is supported by the skeleton and the pore water in the porous medium. Therefore, the total stress of porous media includes effective stress and pore water pressure (Shen *et al.* 2007). For isotropic rock, pore pressure can only change its volume but can't change its shape, and therefore shear stress of the porous medium does not affect the pore pressure. Namely the pore pressure has the same effect with normal stress in all direction. The principle of effective stress in reservoir can be expressed as follows

$$\sigma_{ij} = \sigma'_{ij} + \alpha p \delta_{ij} \quad (2)$$

where σ_{ij} is total stress in the porous media, σ'_{ij} is effective stress, p is the pore pressure, which can be calculated from Eq. (1), δ_{ij} is the sign of Kroneker; α is Biot constant.

According to elastic mechanics (Xu *et al.* 2003), and the Eq. (2) is considered, the equilibrium equation can be deduced as follows

$$\frac{\partial \sigma'_{ij}}{\partial x_j} + \frac{\partial p}{\partial x} - f_{x_i} = 0 \quad i, j = 1, 2, 3 \quad (3)$$

where x is the coordinate, m; f_{x_i} is the body force, N/m³.

The equilibrium equation can be expressed with displacement by substituting the constitutive equations of rock masses and geometric equation into equilibrium

equation as follows

$$G\nabla^2 u_i - (\lambda + G) \frac{\partial \varepsilon_v}{\partial x_i} - \frac{\partial p}{\partial x_i} + f_{x_i} = 0 \quad i = 1,2,3 \quad (4)$$

where λ and G are lame constant; ε_v is volumetric strain and

$$\varepsilon_v = -\left(\frac{\partial u_i}{\partial x_i} + \frac{\partial u_j}{\partial x_j} + \frac{\partial u_k}{\partial x_k}\right)$$

2.3 Coupling relationship and solution route

The relation for porosity of rock mass changing with pore pressure can be expressed by coefficient of compressibility.

$$C_R = \frac{1}{\varphi} \frac{\partial \varphi}{\partial p} \quad (5)$$

where C_R is the coefficient of compressibility of the rock mass, kPa^{-1} .

By separation of variables, the following formula can be obtained

$$C_R \partial p = \frac{\partial \varphi}{\varphi} \Rightarrow \int_{p_0}^p C_R \partial p = \int_{\varphi_0}^{\varphi} \frac{\partial \varphi}{\varphi} \Rightarrow C_R (p - p_0) = \ln \frac{\varphi}{\varphi_0} \quad (6)$$

$$\varphi = \varphi_0 e^{C_R(p-p_0)} \quad (7)$$

According to Ayub's (2016) research, the permeability tensor is no longer a constant with the change of porosity but a function of the porosity because of the reservoir deformation.

In the fluid-solid coupling of reservoir, the relation between permeability tensor and pore pressure always can be built by permeability test under overburden pressure. The empirical equation shown as follows can express the relation between the permeability tensor and deformation of pore.

$$K_{ij}(\Delta \varphi) = K_{ij}^0 \exp[-\alpha \Delta \varphi] \quad (8)$$

where K_{ij} is permeability tensor, $\Delta \varphi$ is the increment of porosity.

In order to realize the process of simulating the interaction of seepage and stress, based on the relationship of pressure, stress and permeability in Eq. (8), and the principle of effective stress in reservoir described in Eq. (2) was also taken into account, we established a interface to deal with the parameters conversion between seepage field and stress field, the main function of the subroutine is to calculate the permeability of each cell by Eq. (8), this program was based on the USDFLD (User subroutine to redefine field variables at a material point) subroutine in Abaqus, we used it to revise the permeability of each grid and then export the new value as the updated permeability in the simulation of seepage with Eclipse. At the same time, we created a program to extract pressure and stress of each block to be imported into Abaqus and Eclipse respectively, the main function of this program is to translate the

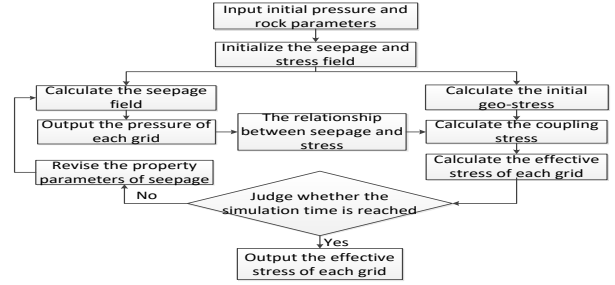


Fig. 2 The route of simulating the development of reservoir considering the seepage and mechanics coupling

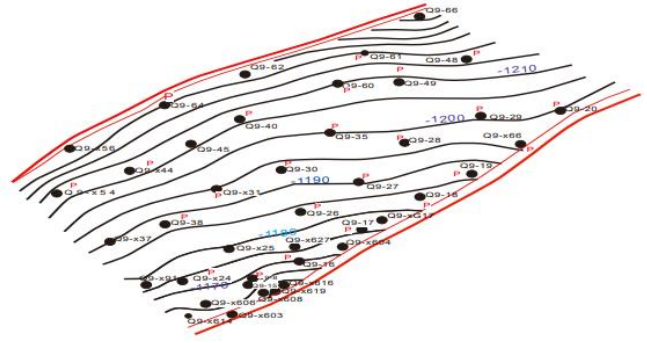


Fig. 3 The top depth and distribution of wells for block Q9G3

geologic model from petrel into finite element model that can be recognized by Abaqus. In the simulation of water flooding, the wells are simplified as structural element, which can be simulated with rebar element in Abaqus. Therefore, by the interface, subroutines and software, we can simulate the development of reservoir with the seepage-mechanics coupling being taken into account. The route of the process is given out in Fig. 2.

3. The establishment of the numerical model

3.1 Geological model

According to the simulation district and the well log data of this project, the Petrel software was employed to build the geological model of Q9G3 block. These log data and geological survey are illustrated below.

First of all, the Q9G3 block belongs to the braided river sedimentary system, because this block is shallow buried reservoir. The characteristic of this block is as follows, the reservoir property is good, the main lithology is fine sandstone and pebbled sandstone. The average porosity is 29.1%, average permeability is $345.31 \times 10^{-3} \mu\text{m}^2$, average content of clay is 8.7%. The size of median particle is 0.17 mm, the sorting coefficient is 1.73. According to the experiment of cores from Jibei oilfield corporation, the formation has strong sensitivity of permeability to water and stress.

The contour map of top depth for the Q9G3 block is shown in Fig. 3, the blue numbers in the figure are the elevation value, the black circles are the well symbol, and the characters beside the circle are the original well names,

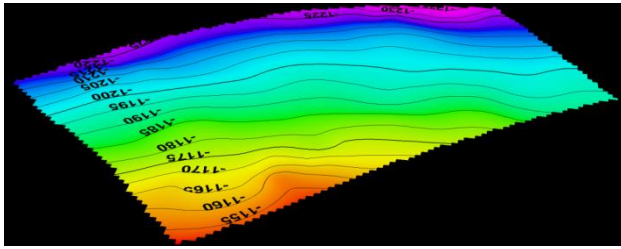


Fig. 4 The DEM model for the top of reservoir

Table 1 Well top data (unit: m)

	G31	G32	G33	G34	G35	base
Q9-20	1130.4	1150.3	1167.0	1184.4	1199.9	1220.0
Q9-48	1034.6	1073.9	1114.5	1155.7	1204.1	1242.1
Q9-X68	1162.2	1181.0	1202.8	1224.4	1238.8	1249.9
Q9-29	1153.8	1189.2	1213.0	1231.4	1249.4	1270.9
Q9-49	1058.5	1108.6	1154.2	1190.5	1213.8	1235.9
Q9-61	1208.3	1233.4	1258.5	1283.7	1308.8	1333.9
Q9-19	1047.5	1083.7	1121.7	1160.2	1192.1	1221.4
Q9-28	1106.3	1153.5	1183.0	1206.4	1227.3	1251.4

where the numbers in the form above are the top depth of each layer, such as G31, G32, etc. The name “base” is the bottom depth of the formation. Therefore, each name G31, G32... is corresponding to each depth value, we can use these names to represent these depths, and vice versa

Table 2 Porosity of well log data

	G31	G32	G33	G34	G35	base
Q9-20	0.309	0.349	0.366	0.261	0.399	0.342
Q9-48	0.314	0.239	0.302	0.317	0.315	0.335
Q9-X68	0.301	0.338	0.329	0.294	0.315	0.351
Q9-29	0.267	0.234	0.279	0.296	0.279	0.238
Q9-49	0.266	0.283	0.232	0.250	0.219	0.320
Q9-61	0.297	0.282	0.300	0.263	0.293	0.253
Q9-19	0.377	0.286	0.330	0.357	0.418	0.332
Q9-28	0.248	0.305	0.314	0.266	0.305	0.300

where the number in the form above is the porosity of each corresponding depth in the reservoir, each top name here represent a depth in Table 1.

Table 3 Permeability of well log data(unit: $\times 10^{-3} \mu\text{m}^2$)

	G31	G32	G33	G34	G35	base
Q9-20	310.24	519.91	650.00	150.03	949.98	899.92
Q9-48	130.00	29.95	330.05	140.06	380.00	259.55
Q9-X68	239.46	610.43	430.72	379.52	159.78	977.00
Q9-29	219.88	90.36	200.03	270.07	280.12	100.15
Q9-49	29.93	90.36	79.82	39.91	19.96	180.72
Q9-61	50.07	29.93	59.87	29.93	109.94	100.15
Q9-19	1840.34	340.36	360.43	910.62	1029.14	460.83
Q9-28	129.52	360.43	370.48	189.76	330.31	270.07

these names are defined by the workers from Jibei oilfield

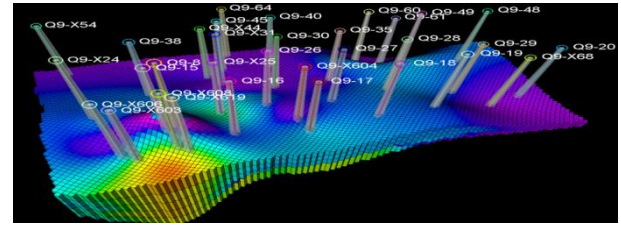


Fig. 5 The 3D geological model of Q9G3 block

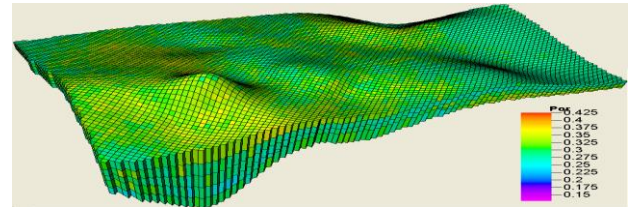


Fig. 6 The 3D porosity model of Q9G3 block

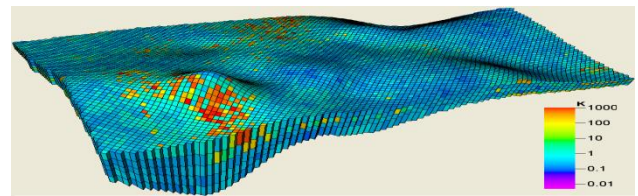


Fig. 7 The 3D permeability model of Q9G3 block

Table 4 Physical and mechanical parameters of the casing, cement ring and formation

	E (Pa)	ν	C (Mpa)	ψ (°)	Uniaxial compressive strength (Mpa)
casing	2.0×10^{11}	0.33	--	--	700
cement ring	3×10^{10}	0.26	26.3	12.8	100
sandstone	2×10^{10}	0.24	20.7	18	80
mudstone	9×10^9	0.35	18.6	20.2	65

where E is the Modulus of elasticity, ν is the Poisson ratio, C is the Cohesion and ψ is the angle of internal friction

corporation.

The contour map above was digitized and then imported into the Petrel2008. The interpolation function in petrel was used to get the elevation everywhere (each grid point) of the top of reservoir, the final rendered and digitized elevation model (DEM) is shown in the Fig. 4

The next work is to use the logging data of some typical wells to obtain the geological model including the structure and property model. The main logging data is comprised of well top and well log data, they are demonstrated in Tables 1-3.

Based on the well top data above, we used the interpolation method with Arithmetic average algorithm to get the top depth of each layer. The route is that the top depth of the reservoir plus the thickness of each grid point equals the bottom depth of the first layer, then the bottom depth of first layer adds the thickness of the second layer equals its bottom depth, the same is other layers.

Likewise, we used the interpolation method to get the porosity and permeability of each grid point to build the property model, the difference was that the properties were calculated with geometry average algorithm.

The final structure and property model are shown in Figs. 5-7.

The number of grid in the *x* and *y* direction are 131 and 111 respectively. The model is divided into five layers in the vertical direction. The total number of grid is 72705 and average effective thickness is 21 m.

In order to finish the coupled simulation of seepage and stress, we need some basic parameters of reservoir rock, these data was provided by the Jibei oilfield corporation, the main mechanical parameters are shown in Table 4.

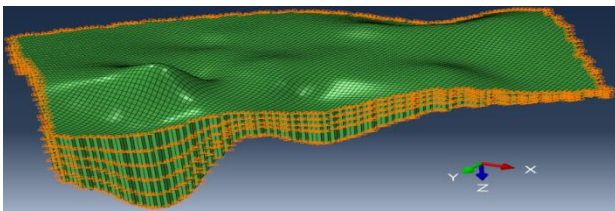


Fig. 8 The constraint boundary of the reservoir

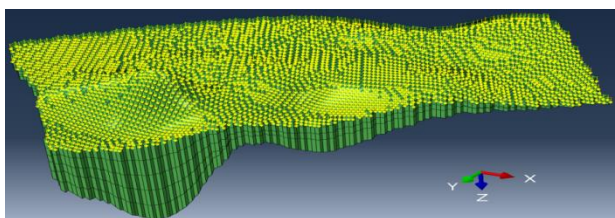


Fig. 9 The load on the top surface of the reservoir

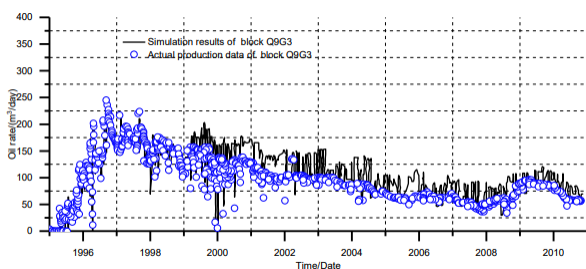


Fig. 10 Fitting results of daily oil

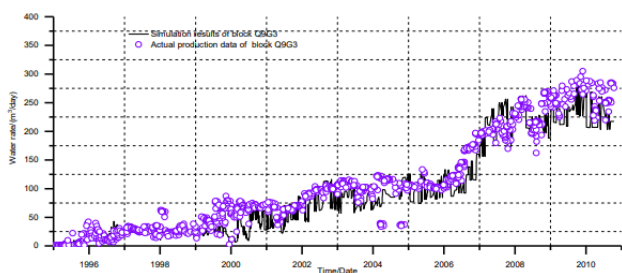


Fig. 11 Fitting results of daily water

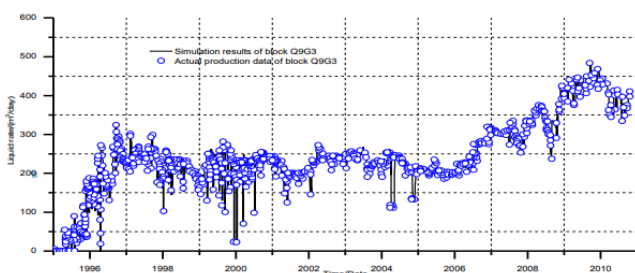


Fig. 12 Fitting results of daily liquid

3.2 Initial and boundary conditions of the numerical model

The initial and boundary conditions of stress field are as follows.

Stress boundary: the bottom surface is constrained in Z direction, and displacement of surrounding is constrained in horizontal direction, which is shown in Fig. 8.

In order to simulate the gravity effect, we calculated the vertical load by the weight of rock overburden, the formula is $\sigma_z = \rho_{rock}gh$, the average weight of the rock is about 24.9MPa, which was set as the vertical load acting on the top surface of the reservoir shown in Fig. 9.

Initial conditions of stress field, as the geo-stress is affected by tectonic movement, which will bring tectonic stress and must be taken into account in the simulation of geo-stress. According to the statistics survey and measurement in-situ of geo-stress in Jibei oilfield, the relation between the horizontal maximum compressive stress and the depth is $2.5+0.0226h$ MPa; The relation between the horizontal minimum compressive stress and the depth is $1.5+0.015h$ MPa. Through the calculation of stress with depth, the maximum horizontal stress in-situ is 29.6 MPa and the minimum horizontal stress in-situ is 19.5 MPa.

The initial oil saturation is 0.65, the initial pore pressure is 12.5 MPa. The fluid can not go through the top and bottom of the model. and there is no mass transferring at the surrounding surface. Therefore, the flow rate at the top and bottom surface is zero.

The injection well is set as fixed flow rate, which is at the range of 30 m³/day to 120 m³/day. The production well is set as constant bottom hole pressure, which is at the range of 2 MPa to 10 MPa.

4. Numerical simulation of fluid-solid coupling for Q9G3 block

4.1 History match of production

There are 28 production Wells in the block and they were open on January 1, 1995, then closed on March 31, 2011. The results of daily oil, daily water and daily liquid are shown as follows in Figs. 10-12. In these figures, the legend “actual production data of Block Q9G3” represent the actual production data from Jibei oilfield corporation, which are marked with blue circle points, the red line is the simulation results.

From the figures above, it can be seen that the calculation results of production match very well with the actual data, which indicates that the mathematical model, numerical model and the solution method established above are correct. The precision of the calculation is shown in Table 5.

Table 5 Fitting precision

	Cumulative fluid (10 ⁴ m ³)	Cumulative water (10 ⁴ m ³)	Cumulative oil (10 ⁴ m ³)
Actual value	123.38	65.13	58.26
Calculation result	122.11	63.56	59.13
Relative error (%)	1.0	2.4	1.5

According to the data in the form above, the relative error of the production index by simulation is less than 5%, which meet the calculation requirement of petroleum industry. Therefore, the mathematical model and the simulation results can be used to analyze the seepage field of this reservoir. The numerical model could be used to conduct coupled simulation of stress and seepage field, and hence to get accurate results.

4.2 Analysis on the casing damage and geo-stress

In order to demonstrate the variation of stress field for Q9G3, the simulation results of the stress of the 1st layer at different time are shown in Figs. 13(a) and 13(b). The two figures as follows are about the displacement distribution in the x direction, which indicates obvious variation trend.

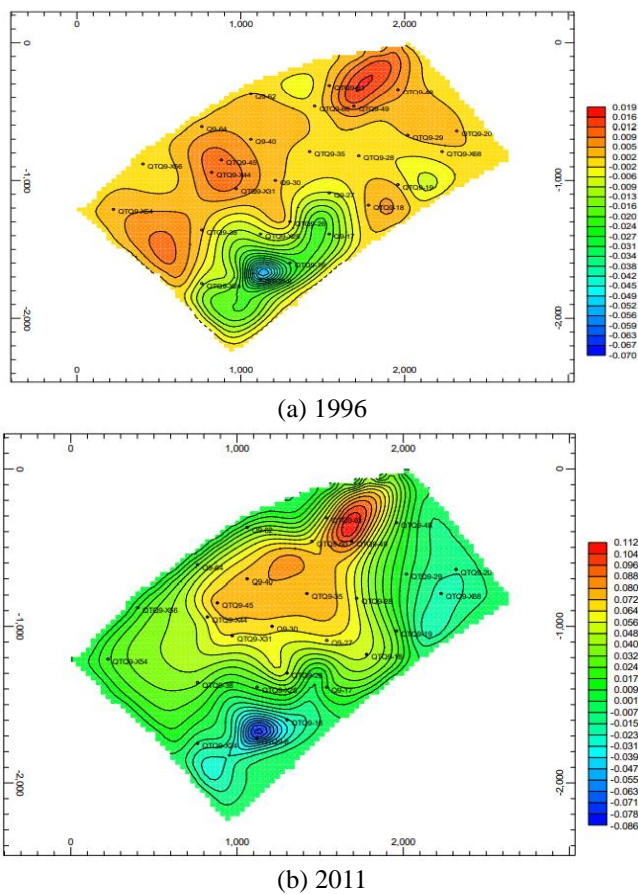


Fig. 13 Displacement in x direction (unit, m)

Table 6 Wells with casing damage problem in Q9G3 block (from Jibei oil field corporation)

number	Well name	Start time	Damaged time	Span (year)	Type of damage	Location of damage	Present status
1	Q9-8	1995	2006	11	necking	Oil layer	Recovering after repair
2	Q9-35	1995	2006	11	broken	Oil layer	Recovering after repair
3	Q9-40	1995	2008	13	necking	Oil layer	Recovering after repair
4	Q9-X44	1995	2008	13	broken	Oil layer	Recovering after repair
5	Q9-45	1997	2002	5	broken	Oil layer	Recovering after repair
6	Q9-49	1995	2004	9	faulted	Oil layer	Recovering after repair
7	Q9-61	1995	2005	10	broken	Oil layer	Recovering after repair

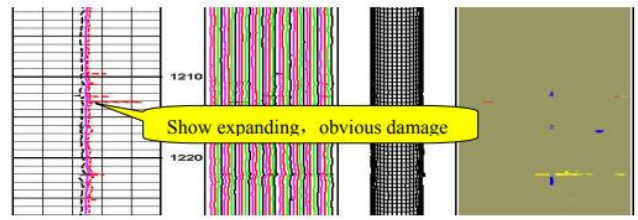


Fig. 14 Result of image processing in abnormal position of caliper for well Q9-8

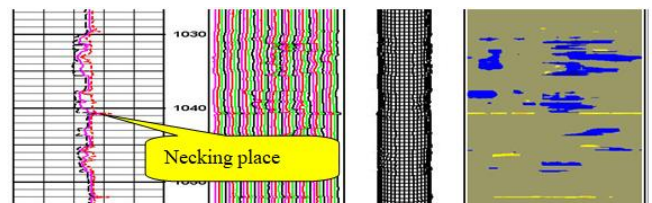


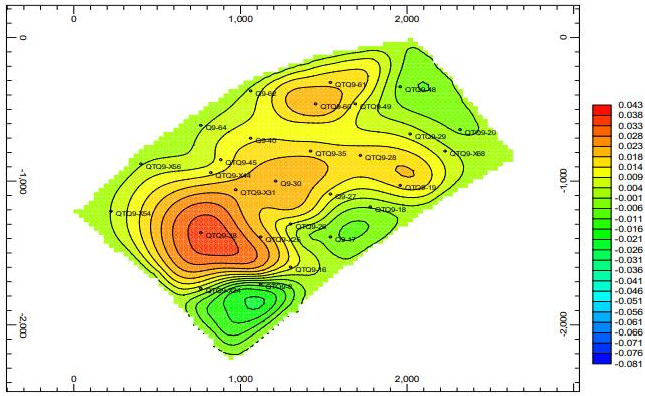
Fig. 15 Result of image processing in abnormal position of caliper for well Q9-61

From Fig. 13(a) and 13(b), the displacement of reservoir in x direction increases gradually after the oil and water are extracted. According to the calculation results, the total horizontal displacement is also increasing, especially near the wells, where the change of the displacement is most obvious. The stress and displacement are generally corresponding to each other, according to the boundary condition of the stress field, the stress concentration happens near the wells during the development of reservoir. This kind of phenomenon is especially obvious for some wells, such as Q9-8, Q9-61, Q9-49, Q9-45, Q9-35 (In the simulation, the prefix “QT” was added to the names of some wells for convenience of summarizing the production index). The displacement of the formation near the well Q9-45, Q9-35, Q9-40 is about 0.10 m, while the deformation near the well Q9-61 is about 0.11 m, the displacement of the formation near the well Q9-8 is about 0.08 m and the direction is on the contrary to the region above. On the whole, this deformation region is forming some deformation concentration zones, which may be likely to become a risk area of casing damage. According to the monitoring data of casing deformation for Q9G3 block, there had been casing damage problem among these wells, which is shown in Table 6 below. The trend indicated by the simulation results matched well with the field data.

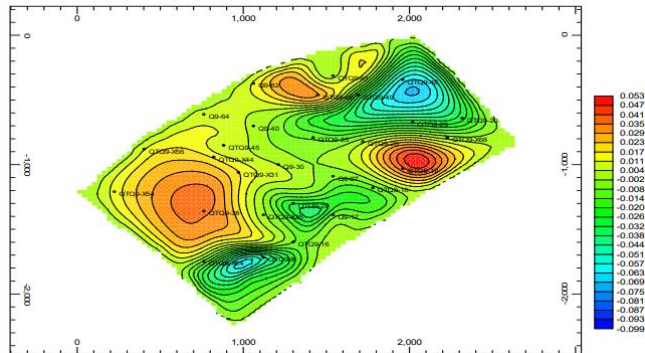
We also got some images of wells with casing damage problem, these images provided by Jibei oilfield were produced and interpreted from seismic test.

As can be seen from Figs. 14 and 15, the wells Q9-8 and Q9-61 are deformed seriously, which matched well with the stress field calculated by our mathematical model and simulation method.

We have checked the bottom hole pressure (BHP) of these production wells with casing damage and find that they are always less than 3 MPa, and even more less than 2 MPa to get more oil rate, this may be a cause for the casing damage problem. Therefore, we’d better not set the BHP to be too low to get more petroleum and should reduce the BHP step by step, so as to keep safe production of wells. The BHP the production well should be reduced step by

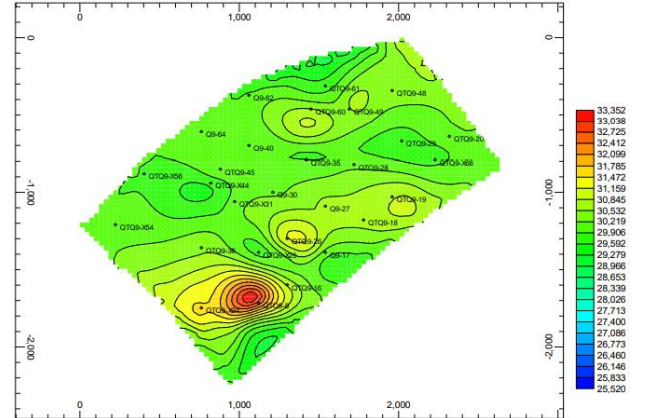


(a) 1996

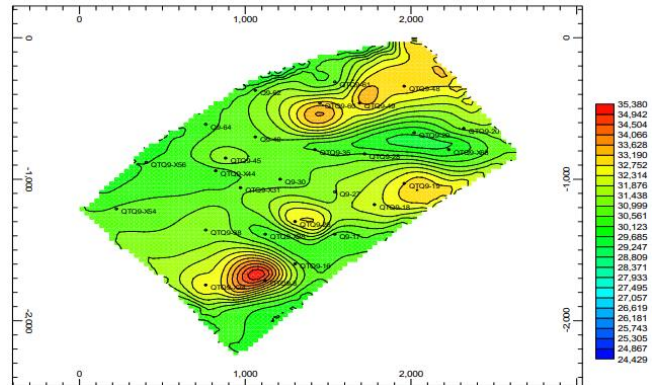


(b) 2011

Fig. 16 Displacement in y direction (unit, m)

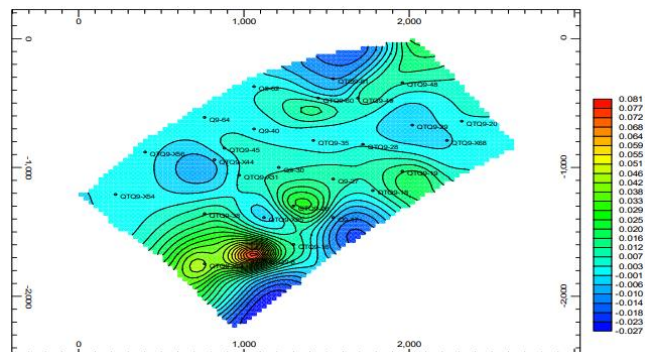


(a) 1996

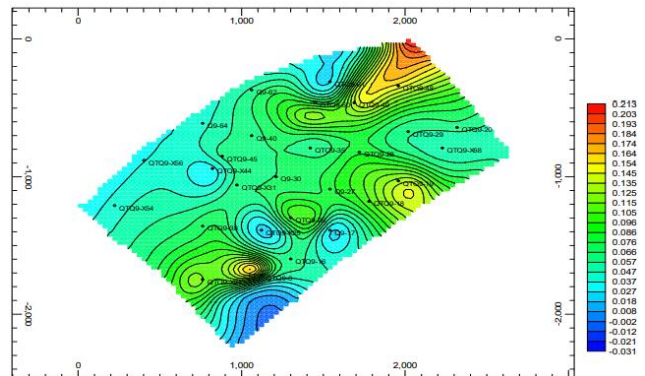


(b) 2011

Fig. 18 Stress distribution in y direction (unit, kPa)



(a) 1996



(b) 2011

Fig. 17 Displacement in z direction (unit, m)

adopted by Jibei oil field corporation in 2012, and the casing damage problem was controlled somewhat. Compared with 2011, the number of well with casing damage had been reduced by 15% in 2012.

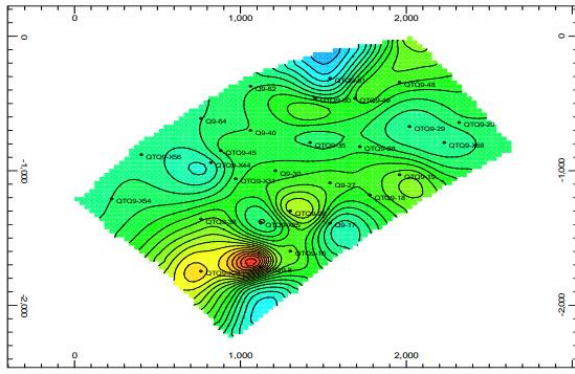
The displacement results in y direction are also given out as follows in Figs. 16(a) and 16(b).

From Figs. 16(a) and 16(b), it can be seen that the displacement in Y direction increases gradually, which is the same as in X direction, it can be inferred that the total horizontal displacement is also increasing, the maximum displacement near well Q9-19, Q9-38, Q9-60 is close to 0.053 m in the Y direction. However, the maximum displacement of Q9-48 is 0.069 m in the negative direction of Y axis, which indicates its casing pipe is bearing heavy load. This may be caused by injecting water with high pressure, and would also probably result in casing damage.

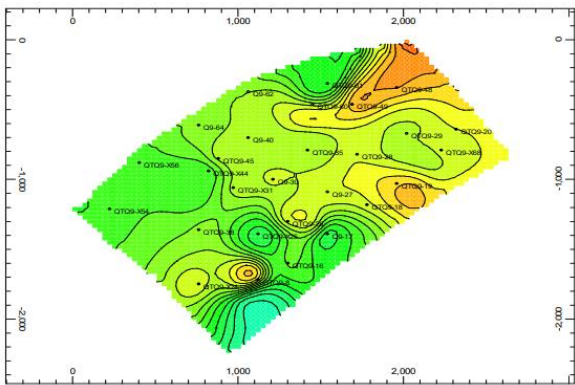
The displacement in z direction is shown in the Figs. 17(a) and 17(b).

The results from Figs. 17(a) and 17(b) indicates that the displacement of z direction also increases gradually with the development of reservoir. The displacement in z direction of the formation near the well Q9-8 is about 0.12 m, the maximum displacement is about 0.21 m, which occurs in the region near the well Q9-48, the direction of these displacement is downward. In some area, the direction of the z displacement is upward, such as the well Q9-61, Q9-17 and Q9-X44, the value is about 0.03m, this may be caused by water injection, these wells had been changed to injection well in the process of production. Finally, it is shown that the displacement of the formation is vertically

step with small interval, such as 0.1 MPa per day to keep a stable oil rate and safe production. This suggestion had been

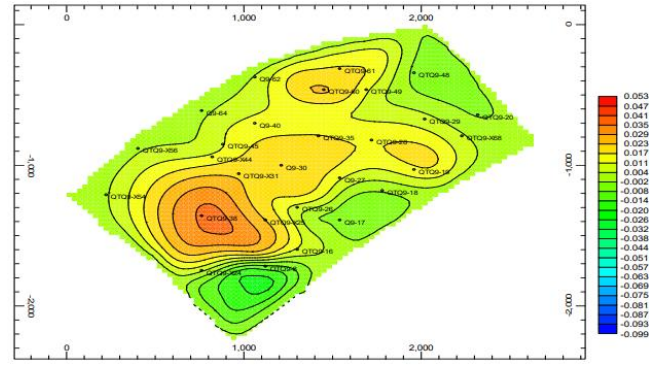


(a) 1996

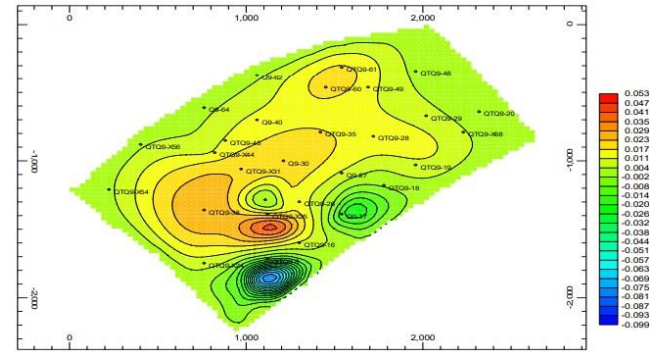


(b) 2011

Fig. 19 Stress distribution in z direction, the upper is in 1996, the lower is in 2011 (unit, kPa)

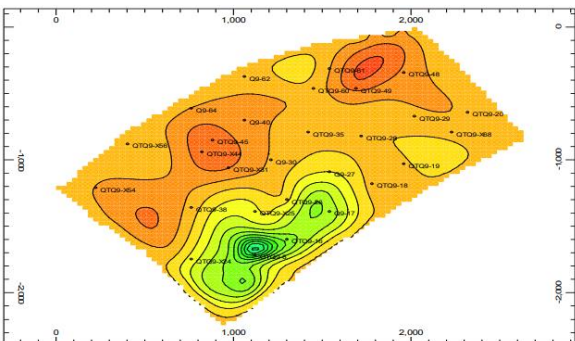


(a) 1st layer

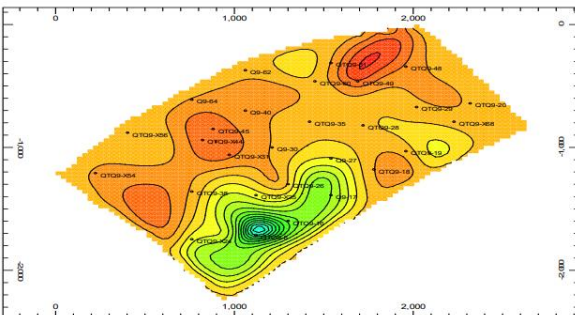


(b) 2nd layer

Fig. 21 The comparison of displacement in y direction for adjacent layer in 1996, the upper and the lower shows displacement of the 1st and 2nd respectively (unit, m)



(a) 1st layer



(b) 2nd layer

Fig. 20 The comparison of displacement in x direction in 1996, the upper and the lower shows displacement of the 1st and 2nd respectively (unit, m)

downward and we can infer that the rock skeleton of

reservoir will sink after a period of production time.

From the simulation results of stress and seepage field, the displacement and its direction are changing, which is characterized in regional distribution. It is mainly controlled by the change of flow field.

Corresponding to the displacement, the stress distribution in y direction is shown as follows in Figs. 18(a) and 18(b).

From Figs. 18(a) and 18(b), the stress in y direction is increasing. During the development of oilfield, the main factor which affects the stress is seepage field. Stress concentration happens near the wells Q9-8, Q9-19, Q9-26, Q9-48, Q9-49 and Q9-60, and the stress of the formation near these wells are about 34.9 Mpa, 32.7 MPa, 32.3 Mpa, 33.6 MPa, 34.1 MPa and 33.1 MPa respectively, which obviously makes up some stress concentration zones. The varied stress concentration near these production wells may lead up to uneven concentrated load on casing pipe, and finally bring casing damage problem to them.

The stress distribution in z direction at different time is demonstrated in the Figs. 19(a) and 19(b) as follows.

As can be seen from Figs. 19(a) and 19(b), the stress in z direction of the formation near the wells Q9-48, Q9-19 and Q9-8 are 33.2 MPa, 31.7 MPa and 30.7 MPa respectively. With the development of the reservoir, the stress in z direction is increasing, which has the same trend with that in y direction.

According to the logging information of Jibei oilfield, there are many mudstone layers in the strata. Bibulous mudstone will swell and the intensity drop sharply when it is soaked in water. This phenomenon is inevitable during

the development of reservoir, under the condition of the same geo-stress, mudstone will firstly yield, the load on the mudstone will be transferred to the casing pipe and may probably cause the casing damage, which is in the form of faulting the pipe.

To analyze the impact of the relative displacement of formation on casing damage, the displacement distribution of adjacent layers are shown in Figs. 20 and 21.

From Figs. 20 and 21, the displacement in the x direction of the formation for the first layer near the well Q9-19 is 0.003 m, while the displacement at the same place for the second layer is about 0.001 m and its direction is on the contrary. The average x displacement around the well Q9-8 for the 1st layer and the 2nd layer are -0.05 m and -0.06 m, which shows difference of horizontal displacement between adjacent layers. The displacement in y direction around the well Q9-61 and Q9-8 also indicates obviously difference between the 1st and the 2nd layer of the formation, the displacement value of the 1st layer near the well Q9-61 is about 0.029 m, while the displacement at the same place for the 2nd layer is about 0.011 m. The displacement of x and y direction in adjacent layers shows significant difference during the early period of development. The difference in the two directions is especially obvious near the production wells where the displacement is larger than that of other places of the reservoir. Different displacement at different places in the axial direction for the same well would probably cause tensile load on the casing pipe. When the difference of displacement between adjacent layers reach to certain value, the tensile load on the casing may exceed its tensile strength, tensile failure will happen at this moment.

5. Conclusions

The mathematical model for injection-production process of reservoir considering Seepage and stress coupling has been built and solved by combination of Eclipse and Abaqus software. The geology model and numerical model for development have been built based on geological survey data in Q9G3 blocks of Jibei oilfield. The development process of the well group is simulated. According to the results of numerical simulation, the main conclusions are drawn as follows.

- With the development progresses, displacement of formation in x, y direction and the total horizontal displacement is increasing, especially near the well places. There has been obvious stress concentration around the production wells, such as Q9-8, Q9-19, Q9-26, Q9-48, Q9-49 and Q9-60, etc. The displacement at the places near these wells is distinctly higher than other area. The trend of distribution of displacement illustrated by simulation results match very well with the monitoring data and casing damage situation.

- During the development of Q9G3 block, the final displacement in z direction is downward. The vertical displacement will cause the rock skeleton of reservoir to sink, which will produce tensile load in axial direction on the casing pipe and negative influence on the environment of the ground surface.

- Displacement in x, y and z direction of adjacent layers of formation are significantly different, especially near the producing wells, where the displacement is larger than in other places. Due to this difference, tensile load on the casing pipe may exceed its tensile strength and hence tensile failure will happen in this situation.

- For the production well, the bottom hole pressure should not be set too low, we can reduce the bottom hole pressure of the production well gradually, for instance 0.1 MPa once, so as to keep safe production and get high productivity, the injection pressure for water well should not be higher than the cracking pressure of rock to prevent expanding of well neck.

Acknowledgements

This work was financially supported by Natural Science Foundation of China (Grant No. 41702340), the open fund project (Grant No. ESP1406) from Ecological Security and Protection Key Laboratory of Sichuan Province (Mianyang Normal University), the open foundation project from State Key Laboratory of Oil and Gas Reservoir Geology and Exploitation of Southwest Petroleum University (Grant No. PLN1131), the open foundation project (Grant No.2016trqdz02) from Sichuan Key Laboratory of Natural Gas Geology, the project (Grant No. 2014QH036) from sail plan of Southwest Petroleum University, the project (No. 2014_3310, 2014_3334) from Work Safety Supervision Bureau of China and open foundation project from State Key Laboratory for Geo Mechanics and Deep Underground Engineering in China University of Mining & Technology (Grant No.SKLGDUK1308), the major projects of national science and technology(Grant No.2017ZX05013-001, 2017ZX05013-006 and 2017ZX05037-001). All the data in this manuscript provided by Jibei Oil Field Corporation is greatly appreciated.

References

- Ai, C. (2003), "Mechanism and theoretic models of casing failure and numerical calculations with them", Ph.D. Dissertation, Daqing Institute of Petroleum, Daqing, China.
- Ayu, E., Kamran, G. and Hamid, H. (2016), "A coupled geomechanical reservoir simulation analysis of CO₂, EOR: A case study", *Geomech. Eng.*, **10**(4), 423-436.
- Bu, X.Y., Dang, X.G. and Zhang, J. (2011), "Casing failure mechanism and modeling method", *J. Hebei Polytech. Univ.*, **33**(3), 122-124.
- Cheng, L.S., Luo, Y.Y. and Ding, Z.P. (2013), "Fuzzy comprehensive evaluation model for estimating casing damage in heavy oil reservoir", *Petrol. Sci. Technol.*, **31**(10), 1092-1098.
- Cui, X.B., Yue, B.Q., Luo, W.D. and Zhang, H. (1994), "A prediction method for casing damage wells of oilfield with water-injection", *J. Univ. Petrol. Chin.*, **18**(1), 50-55.
- Diao, S., Yang, C.H., Liu, J.J. and Huang X.N. (2008), "Mechanism of seepage induced casing damage and numerical simulation", *Rock Soil Mech.*, **29**(2), 327-332.
- Han, X.T., Liang, G.P., Wu, E.C., Qian, H.S. and Zhou, Y.F. (2006), "Oil field numerical simulation for the casing damage of software development and application", *Digit. Petrol. Chem.*

- Ind.*, **4**(1), 32-36.
- Huang, X.L., Liu, J.J., Yang, C.H. and He, X. (2008), "The fluid-structure coupling bet well sidewall stability studies", *Oil Drill. Prod. Technol.*, **30**(6), 83-87.
- Koltuk, S., Fernandez-Steeger, T.M. and Azzam, R. (2015), "A numerical study on the seepage failure by heave in sheeted excavation pits", *Geomech. Eng.*, **9**(4), 513-530.
- Liu, F., Fu, J.H., Li, Z.X., Sun, K.Z., Lei, M. and Tu, L. (2008), "Geometry mechanical model and calculating analysis of casing wear in deep well", *Oil Field Equip.*, **37**(2), 12-15.
- Raoof, G., Vamegh, R., Bernt, A. and Mojtaba, M. (2016), "Geomechanical and numerical studies of casing damages in a reservoir with solid production", *Rock Mech. Rock Eng.*, **49**(4), 1441-1460.
- Ren, L.H., Wang, F.X. and Liu, J.D. (2010), "Analysis of effect of sand production on casing damage in dagang Gangxi Oilfield", *Oil Field Equip.*, **39**(6), 28-31.
- Shen, X.P., Xi, Y.Y. and Zhang, J.C. (2007), "A dual-porosity finite element formulation for instability analysis of borehole in rock mass", *J. Shenyang Univ. Technol.*, **27**(5), 571-574.
- Wang, T., Yang, S., Zhu, W., Bian, W.J., Liu, M., Lei, Y., Zhang, Y., Zhang, J., Zhao, Wei., Chen, Lan., Zhou, X.P. and Liao, J.H. (2011), "Law and countermeasures for the casing damage of oil production wells and water injection wells in Tarim Oilfield", *Petrol. Explor. Develop.*, **38**(3), 352-361.
- Wei, Z. and Gu, S.Q. (2013), "Casing mechanism of engineering hazards in a oil field in central China", *Environ. Earth Sci.*, **70**(2), 869-875.
- Wu, S.Y., Li, Z.A. and Yin, Z.M. (2005), "Oil and water Wells casing damage types and research methods", *Xinjiang Petrol. Technol.*, **15**(3), 12-14.
- Xu, B.Y. and Liu, X. S. (2003), *Elastic and Plastic Mechanics and Its Application*, Tsinghua University Press, Beijing, China.
- Yin, Z.M., Wu, Q. and Liu, J.J. (2004), "Numerical simulation of geo-stress distribution during injecting well blowout", *Rock Soil Mech.*, **25**(6), 363-368.